REVIEW

The role of disordered protein regions in the assembly of decapping complexes and RNP granules

Stefanie Jonas and Elisa Izaurralde[1]

Department of Biochemistry, Max Planck Institute for Developmental Biology, 72076 Tübingen, Germany

The removal of the 5′ cap structure by the decapping enzyme DCP2 inhibits translation and generally commits the mRNA to irreversible 5′-to-3′ exonucleolytic degradation by XRN1. DCP2 catalytic activity is stimulated by DCP1, and these proteins form the conserved core of the decapping complex. Additional decapping factors orchestrate the recruitment and activity of this complex in vivo. These factors include enhancer of decapping 3 (EDC3), EDC4, like Sm14A (LSm14A), Pat, the LSm1–7 complex, and the RNA helicase DDX6. Decapping factors are often modular and feature folded domains flanked or connected by low-complexity disordered regions. Recent studies have made important advances in understanding how these disordered regions contribute to the assembly of decapping complexes and promote phase transitions that drive RNP granule formation. These studies have also revealed that the decapping network is governed by interactions mediated by short linear motifs (SLiMs) in these disordered regions. Consequently, the network has rapidly evolved, and although decapping factors are conserved, individual interactions between orthologs have been rewired during evolution. The plasticity of the network facilitates the acquisition of additional subunits or domains in pre-existing subunits, enhances opportunities for regulating mRNA degradation, and eventually leads to the emergence of novel functions.

The removal of the mRNA 5′ cap structure by the decapping enzyme DCP2 is a critical step in the post-transcriptional regulation of gene expression in eukaryotes. In contrast to other regulatory mechanisms, such as translational repression and deadenylation, decapping is generally an irreversible process that shuts down translation initiation and exposes bulk mRNA to full degradation by the major cytoplasmic 5′-to-3′ exonuclease XRN1 (Arribas-Layton et al. 2013). Although DCP2 is catalytically active in vitro, its activity is stimulated by additional proteins termed decapping activators or enhancers of decapping (EDCs) (Arribas-Layton et al. 2013).

The best-characterized and most widely conserved decapping activator is DCP1, which, together with DCP2, forms the conserved core of the decapping complex. Additional activators include EDC3, like Sm14A (LSm14A), Pat, the LSm1–7 complex, the RNA helicase DDX6, and the species-specific activators Edc1, Edc2, and EDC4 (Arribas-Layton et al. 2013). The precise molecular mechanism by which most of these proteins facilitate decapping in vivo is unclear. Some of these proteins (such as DCP1, Edc1, Edc2, and EDC3) directly enhance decapping by stimulating DCP2 catalytic activity, whereas other proteins (such as DDX6 and LSm14A) facilitate decapping by inhibiting translation and/or promoting mRNP rearrangements that increase the accessibility of DCP2 to the mRNA cap structure in vivo (Kshirsagar and Parker 2004; Deshmukh et al. 2008; She et al. 2008; Floor et al. 2010, 2012; Nissan et al. 2010; Borja et al. 2011; Fromm et al. 2012; Rajyaguru et al. 2012; Sweet et al. 2012).

DCP2 and decapping activators are characterized by a modular architecture consisting of globular folded domains (Fig. 1, colored regions) connected or flanked by low-complexity regions predicted to lack a defined tertiary structure (Fig. 1, white disordered regions). While the globular folded domains are conserved, the disordered regions diverge considerably in sequence and length among eukaryotes. Recent studies indicate that despite their overall lack of conservation, these disordered regions perform two important functions. First, these regions mediate complex assembly through short linear motifs (SLiMs) (Fig. 1, black vertical bars) that bind to surfaces on the folded domains of their binding partners. Second, they possess intrinsic properties that lead to the formation of large RNP granules (e.g., P bodies, P granules, and neuronal granules) where decapping activators, additional post-transcriptional mRNA regulators, and mRNA substrates accumulate (Eulalio et al. 2007a; Parker and Sheth 2007).

[*Keywords*: DCP2; decapping; mRNA decay; SLiMs]
[1]**Corresponding author**
E-mail elisa.izaurralde@tuebingen.mpg.de
Article is online at http://www.genesdev.org/cgi/doi/10.1101/gad.227843.113. Freely available online through the *Genes & Development* Open Access option.

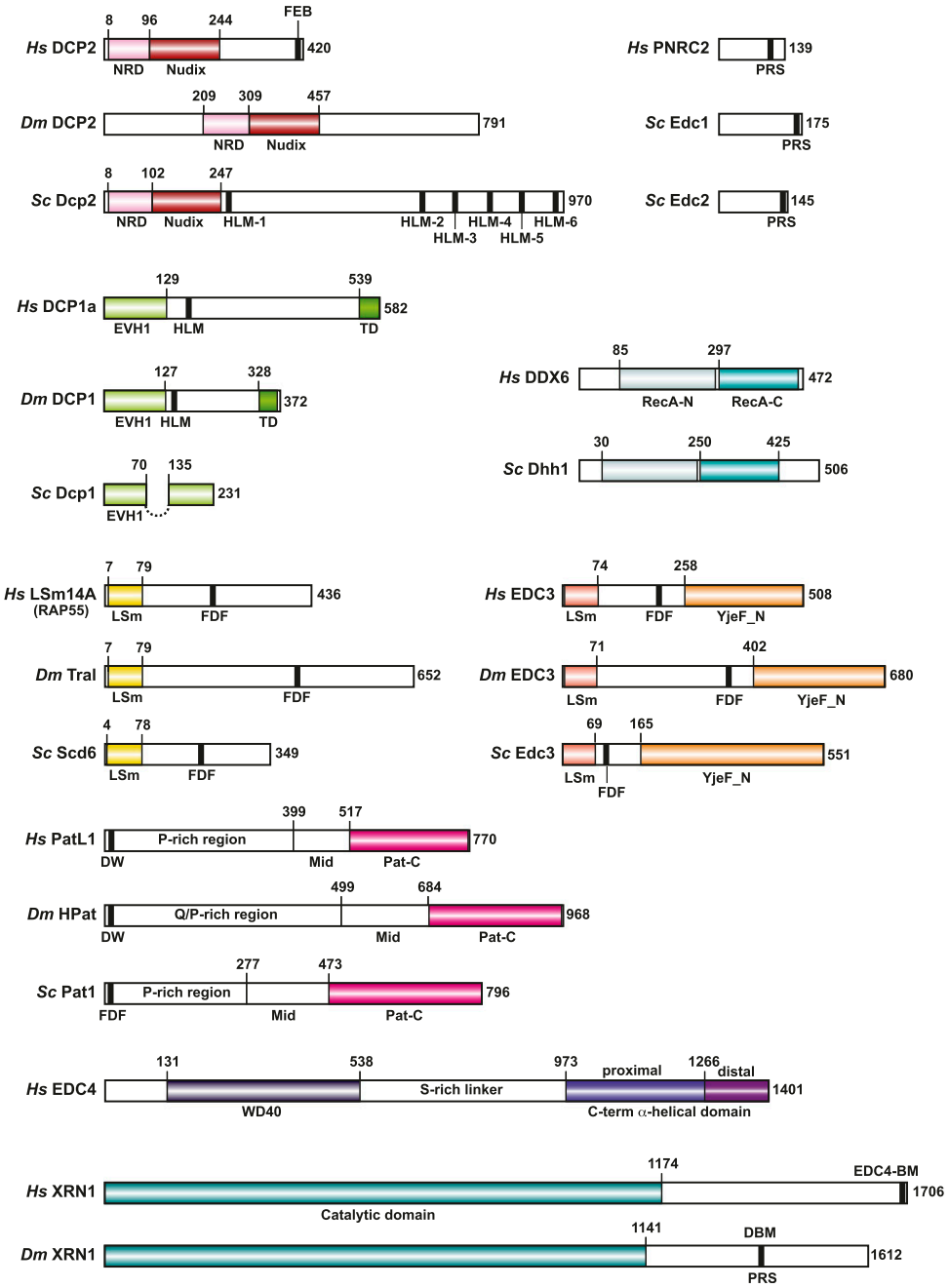

Figure 1. Domain organization of decapping factors. (*Hs*) *Homo sapiens*; (*Dm*) *Drosophila melanogaster*; (*Sc*) *Saccharomyces cerevisiae*. The *Dm* and *Sc* proteins are shown when they significantly differ from the human proteins. The colored regions represent structured domains. The white sectors represent predicted disordered regions. Black vertical lines indicate experimentally validated SLiMs. The numbers *above* the protein schematic represent amino acid positions at fragment boundaries for each protein. The seven LSm proteins (not shown) contain an LSm domain of ~100 amino acids and short N-terminal or C-terminal extensions. (FDF and DW) SLiMs containing the indicated amino acids. EDC4 is also known as Ge-1 or Hedls. DDX6 is also known as RCK and p54. The *Sc* Dcp1 EVH1 domain contains an unstructured insert of 55 residues (dotted line) and is therefore longer than the EVH1 domain of DCP1 proteins in other species (She et al. 2004). The Pat Mid region is predicted to be α-helical but is unfolded in isolation (Braun et al. 2010).

In this review, we describe recent advances in our understanding of how the rapidly evolving disordered regions in decapping factors orchestrate the dynamic assembly and rewiring of the decapping interaction network. Although important new insights into the recruitment of decapping complexes to specific mRNAs by RNA-binding proteins have been provided in recent years (Arribas-Layton et al. 2013), we do not extensively discuss them in this review. Rather, we focus on the interactions among core decapping factors and their assembly into functional

complexes. First, we briefly summarize current models of how the catalytic activity of DCP2 is activated by DCP1. Second, we review the evidence demonstrating that the globular domains in DCP1, EDC3, LSm14A, and DDX6 provide binding sites for SLiMs in disordered regions of their binding partners. Some of these partners compete for binding to a common surface, suggesting that decapping involves sequential and/or mutually exclusive interactions that must be coordinated. Decapping typically occurs on deadenylated mRNAs and is followed by the degradation of the mRNA body in the 5′-to-3′ direction (Arribas-Layton et al. 2013). We emphasize how SLiMs play a role in the coordination of decapping with mRNA deadenylation and 5′-to-3′ mRNA degradation. Finally, we discuss recent evidence indicating that disordered regions promote the assembly of RNP granules, which exhibit the properties of liquid droplets. Although decapping factors colocalize with translational repressors in these granules, mRNAs destined for full degradation or translational repression are correctly identified in the cell. We outline potential molecular mechanisms that allow cells to maintain functional and target specificity.

Because orthologous decapping factors often have different names in different species (e.g., Scd6, Trailer Hitch, CAR-1, RAP55, and LSm14A) or multiple names in the same organism (e.g., DDX6, RCK, and p54), we use the names of the human proteins (Fig. 1) to refer to the protein families and indicate species names to refer to observations that have been reported only in a specific organism.

The decapping interaction network

The globular folded domains present in decapping factors are well conserved, and structural information is available for most of the individual domains except the EDC4 WD40 domain and the proximal portion of its C-terminal α-helical domain (Figs. 1–3). The role of the folded domains is to provide catalytic activity—as in the case of the Nudix domain in DCP2 and the RecA-like domains in DDX6—as well as mediate protein–protein interactions. However, in addition to interactions with other globular domains, which follow the classical principle of mutual recognition by complementary tertiary structures, the folded domains also provide binding surfaces for the SLiMs present in the disordered regions of their binding partners.

SLiM-mediated interactions confer specific properties to the protein interaction network that are distinct from networks governed by globular–globular domain interactions. These properties have been discussed in recent reviews (Davey et al. 2012; Tompa 2012) and are only briefly summarized here. First, SLiMs are short three- to 10-amino-acid motifs present in disordered protein regions. These motifs are largely disordered in the absence of their specific binding partners and adopt defined conformations only upon binding (Davey et al. 2012; Tompa 2012). Consequently, the residues forming the binding interface cannot be predicted in the absence of structural information.

Second, because of the small number of residues that contact the binding partner, SLiMs mediate relatively low-affinity interactions that are transient and can be easily modulated by post-translational modifications (i.e., phosphorylation). Nonetheless, the interactions can be highly specific, and high affinity can be achieved through avidity effects generated by the presence of tandem motifs, by contributions from the flanking disordered regions that extend the interaction interface, or by oligomerization of the binding partners (Davey et al. 2012; Tompa 2012).

Finally, an interesting property of SLiMs is that they are evolutionarily plastic because a few amino acid substitutions are sufficient to disrupt or eventually generate a new motif (Davey et al. 2012; Tompa 2012). Thus, SLiMs are expected to evolve rapidly, particularly because they occur in disordered regions in which amino acid substitutions are tolerated due to the lack of structural constraints to maintain a protein fold. As a result, SLiMs have the propensity to evolve convergently (Davey et al. 2012; Tompa 2012).

DCP1 and DCP2 form the conserved catalytic core of the decapping complex

The decapping enzyme DCP2 belongs to the Nudix family of pyrophosphatases and catalyzes hydrolysis of the cap structure, releasing m^7GDP and a 5′ monophosphorylated mRNA (Lykke-Andersen 2002; van Dijk et al. 2002; Wang et al. 2002). The Nudix catalytic domain is flanked N-terminally by a conserved α-helical regulatory domain (NRD) and C-terminally by a highly divergent extension containing from 176 amino acids in humans to 723 amino acids in *Saccharomyces cerevisiae* (*Sc*) (Figs. 1, 2A; Lykke-Andersen 2002; van Dijk et al. 2002; She et al. 2006, 2008).

DCP1 contains an EVH1 domain consisting of seven β strands arranged into two β sheets (Figs. 1, 2A). The β sheets form a V-shaped β sandwich that is closed on one end by a C-terminal α helix (α2). In addition, the DCP1 EVH1 domain contains an N-terminal α helix (α1), which is unique to the DCP1 protein family (She et al. 2004, 2008). The structure of the *Schizosaccharomyces pombe* (*Sp*) Dcp1–Dcp2 complex demonstrates that this specific helix and a conserved loop in the Dcp1 EVH1 domain interact with the α1 helix of the Dcp2 NRD (Fig. 2A; She et al. 2008).

The structural studies also revealed that the Dcp2 NRD and Nudix domains are connected by a flexible hinge region and can adopt multiple conformations relative to each other. These conformations can be classified as open or closed and likely represent transition states between inactive and active catalysis (Deshmukh et al. 2008; She et al. 2008; Floor et al. 2010, 2012). In the open conformation, the two domains are far apart, and the active site is incomplete. In the closed conformation, the NRD and Nudix domains interact, forming a composite active site (Fig. 2A). Dcp2 closure is promoted by cap analogs and Dcp1, leading to the model that Dcp1 enhances decapping by binding to the NRD and stabilizing the closed Dcp2 conformation (Deshmukh et al. 2008; She et al. 2008). However, how this is achieved in molecular terms remains unresolved (Fromm et al. 2012).

Furthermore, it is not known whether the closed conformation observed in the crystal accurately reflects

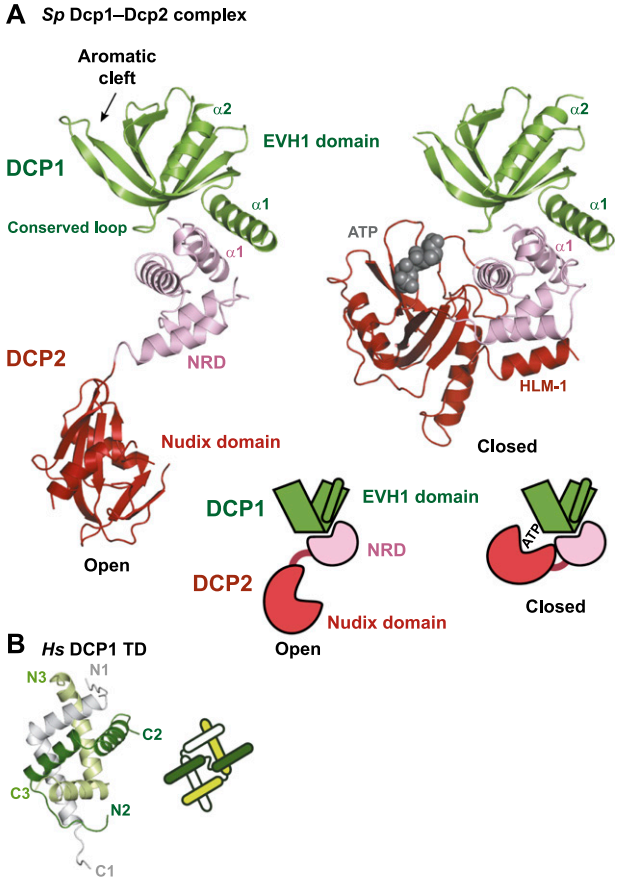

Figure 2. (*A*) Structure of the *Sp* DCP1 EVH1 domain (green) bound to the DCP2 N-terminal domains consisting of a regulatory domain (NRD; salmon) and a Nudix catalytic domain (red) (Protein Data Bank [PDB] code: 2QKM). The flexibility of DCP2 is highlighted by the two conformations found in the crystal structure. The closed conformation has been suggested to resemble the catalytically active form and is crystallized with ATP bound close to the active site (gray). In the close conformation, the HLM-1 helix is bound to the NRD and is therefore inaccessible for EDC3 or LSm14A binding. In the inactive open conformation, the catalytic domain is tilted away from the regulatory domain, and the HLM-1 is not visible. (*B*) *Hs* DCP1a trimerization domain (TD). The three chains are shown in dark and light green and gray, respectively (PDB code: 2WX3).

the catalytically active form of the enzyme because, in this conformation, the residues involved in substrate binding are not clustered (Floor et al. 2010, 2012). These observations suggest that additional enzyme structural states must exist in solution.

Rewiring of the catalytic core of the metazoan decapping complex

Surprisingly, the DCP1 residues mediating the interaction with DCP2 are not highly conserved in metazoans (She et al. 2008). Accordingly, it has been suggested that metazoan DCP1 and DCP2 do not directly interact and that an additional metazoan-specific factor, EDC4, is required to bridge their interaction (Fenger-Grøn et al. 2005; Yu et al. 2005; Xu et al. 2006). Nevertheless, it is possible that, in metazoans, DCP1 and DCP2 interact in a manner structurally similar to that observed in the yeast orthologs, but this interaction might be very weak in the absence of stabilizing partners. Consequently, the interaction might only occur in *cis*; i.e., between DCP1 and DCP2 molecules bound to the same EDC4 scaffold.

EDC4 consists of an N-terminal WD40 domain and a C-terminal α-helical domain, which are connected by a serine-rich linker (Fig. 1; Fenger-Grøn et al. 2005; Yu et al. 2005; Xu et al. 2006; Jínek et al. 2008). The distal portion of the EDC4 C-terminal domain adopts an all α-helical fold, which is similar to the C-terminal domain of Pat (Pat-C) (Fig. 3A–C; Jínek et al. 2008) and structurally related to ARM and HEAT repeat proteins. The proximal portion of the C terminus mediates self-interaction and is predicted to be also α-helical (Xu et al. 2006; Jínek et al. 2008).

The molecular basis for DCP2 and DCP1 interaction with EDC4 has not been fully elucidated, but it is known that these interactions involve the DCP2 and DCP1 regions that are specific to metazoans. For instance, human (*Homo sapiens* [*Hs*]) DCP2 binds the C-terminal α-helical domain of EDC4 through a C-terminal motif that is absent in yeast DCP2 (Fig. 1; Bloch et al. 2011). Based on its amino acid composition, we termed this motif the phenylalanine-rich EDC4-binding (FEB) motif (Fig. 1). Similarly, *Hs* DCP1 interacts with EDC4 through a C-terminal extension that is not present in the yeast proteins (Fig. 1; Tritschler et al. 2009a).

The metazoan DCP1 C-terminal extension is not well conserved, except for a short helical leucine-rich motif (HLM or motif I) and a C-terminal trimerization domain (TD) (Fig. 1, TD; Tritschler et al. 2009a; Fromm et al. 2012). Crystal structures of the *Hs* and *Drosophila melanogaster* (*Dm*) DCP1-TD reveal an anti-parallel assembly comprised of three kinked α helices (Fig. 2B; Tritschler et al. 2009a). DCP1 trimerization is required for its interaction with DCP2 and EDC4 and therefore for efficient decapping in vivo (Tritschler et al. 2009a). The TD could bind DCP2 and EDC4 directly or contribute to binding affinity through avidity effects generated by the multimerization of low-affinity binding sites present in other regions of the DCP1 protein.

Interestingly, Pdc1, a protein with limited similarity to EDC4, is present in *Sp* but not *Sc*. Pdc1 interacts with Dcp2, Dcp1, and Edc3 but is not required for Dcp2–Dcp1 interaction (Wang et al. 2013). The lack of a FEB motif in *Sp* Dcp2 and of a TD in *Sp* Dcp1 indicates that they interact with Pdc1 using a substantially different binding mode.

The acquisition of the EDC4 scaffold and of the C-terminal extension in DCP1, along with the rapid evolution of the DCP2 C-terminal extension and the decreased affinity of DCP1 for DCP2, are indicative of the rewiring of the decapping network in metazoans (Fig. 5, below). Furthermore, the presence of a TD in DCP1 has increased the connectivity and complexity of the network in these organisms, which likely provides additional opportunities for regulating DCP2 activation.

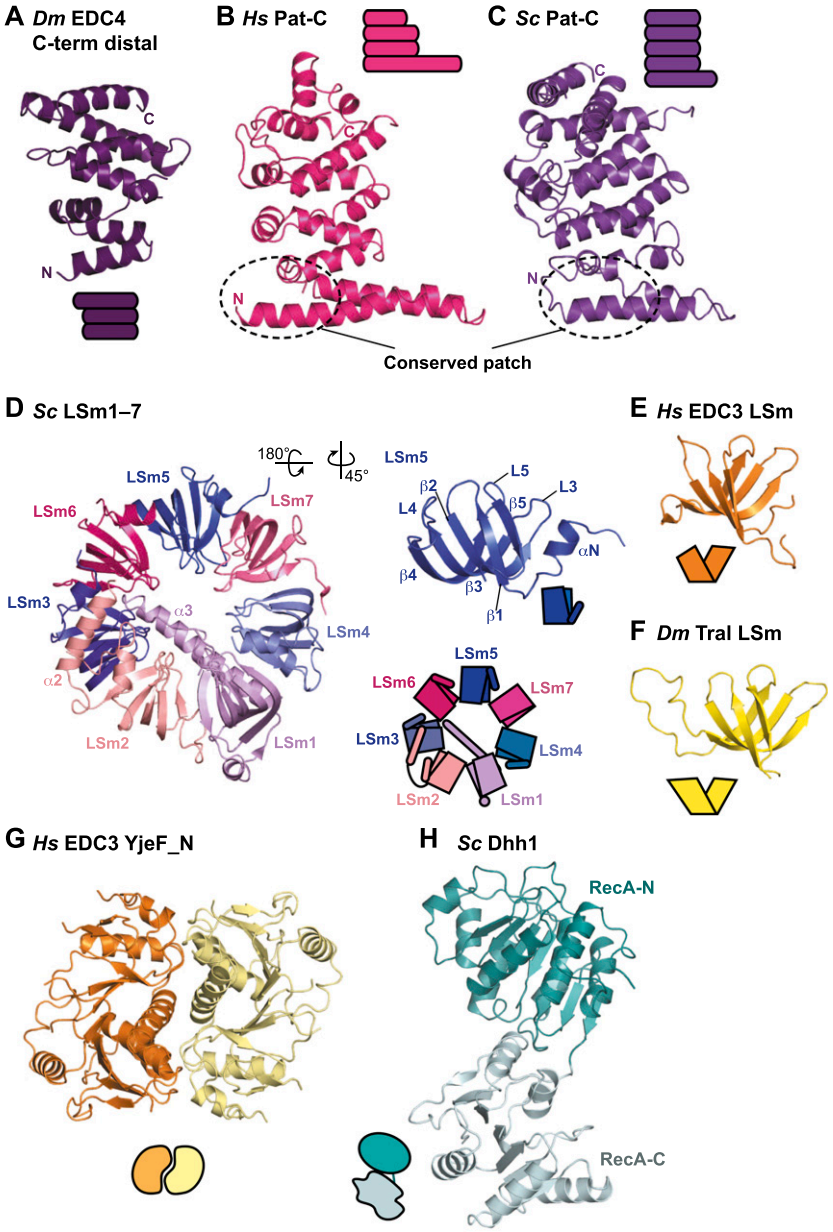

Figure 3. Structures of the folded globular domains of decapping factors. (*A*) Distal portion of the C-terminal domain of *Dm* EDC4 (PDB code: 2VXG). (*B*,*C*) The C-terminal domain of *Hs* and *Sc* Pat (Pat-C). A conserved basic patch is involved in binding to RNA, the LSm1–7 ring, EDC4, and DCP2 (PDB codes: 2XEQ and 4C8Q, respectively). (*D*) Structure of the *Sc* LSm1–7 ring (PDB code: 4C92). On the *right*, LSm5 is shown with secondary structure elements typical for Sm and LSm proteins labeled. (*E*,*F*) Structures of the divergent LSm domains of *Hs* EDC3 (orange) (PDB code: 2VC8) and *Dm* LSm14A (yellow) (PDB code: 2VXE). (*G*) Structure of the C-terminal dimerization domain of *Hs* EDC3. Monomers are shown in orange and yellow (PDB code: 3D3K). (*H*) Structure of *Sc* Dhh1 consisting of two RecA-like domains (PDB code: 4BRU). N and C indicate the N-terminal and C-terminal ends, respectively.

Rewiring of the DCP1 EVH1 domain–ligand interaction network and the emergence of novel functions

In addition to the interface with DCP2, the DCP1 EVH1 domain contains a conserved aromatic cleft that is typically used by EVH1 domains to bind proline-rich (P-rich) sequences (PRSs) in protein ligands (Figs. 2A, 4A,B; She et al. 2004; Braun et al. 2012; Lai et al. 2012). Studies in *Sc*, *Dm*, and *Hs* cells indicate that although the aromatic cleft of the DCP1 EVH1 domain is conserved, it recognizes different PRS-containing ligands in these organisms (Fig. 5). The ligands, on the other hand, have a common PRS that binds the aromatic cleft, but their additional domains are distinct, resulting in the formation of complexes with potentially different functions.

In *Sc*, the aromatic cleft binds PRSs in Edc1 and Edc2 (Figs. 1, 5; Borja et al. 2011), which are absent in metazoans. It has been proposed that after Dcp1 promotes Dcp2 closure, this closed conformation is further stabilized by Edc1, which binds Dcp1 and could contact Dcp2 or the substrate, resulting in synergistic activation of the enzyme (Floor et al. 2012).

In *Dm*, the DCP1 aromatic cleft binds a PRS in the C-terminal region of XRN1 (Figs. 1, 4A, 5, DCP1-binding motif [DBM]) and serves to link decapping with 5′-to-3′ mRNA decay (Braun et al. 2012; see below). In humans, the DCP1 groove binds PNRC2 (Figs. 1, 4B, 5; Lai et al. 2012), which is a vertebrate-specific protein that also enhances decappping activity in vitro. PNRC2 has been proposed to couple decapping with the nonsense-

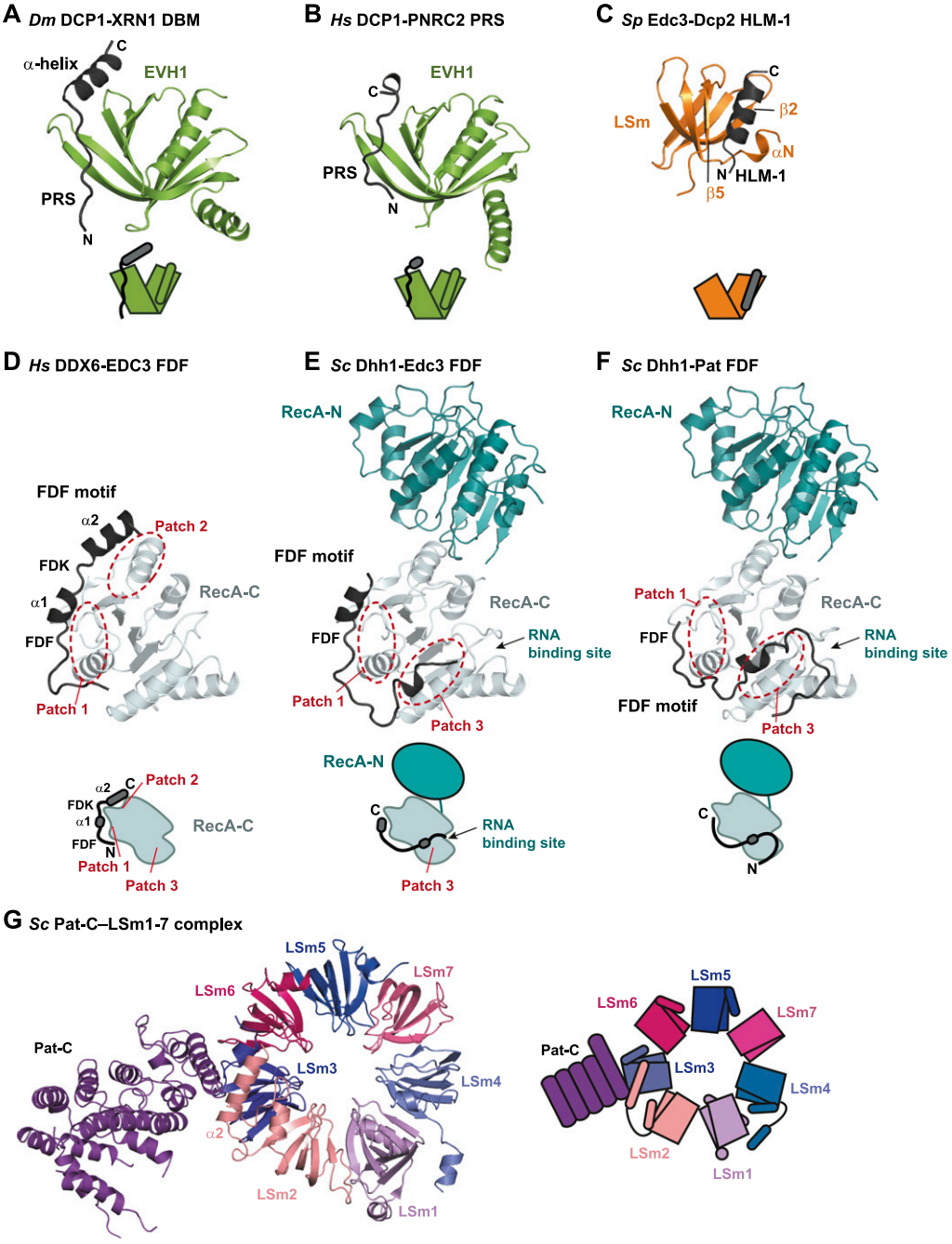

Figure 4. Globular domains in decapping factors mediate protein–protein interactions and provide binding sites for SLiMs. (*A*) The *Dm* XRN1 DBM binds to the DCP1 EVH1 domain. The DBM peptide binds the aromatic cleft and forms an additional helix contacting additional surfaces on the EVH1 domain (PDB code: 2LYD). (*B*) Structure of the PNRC2 PRS bound to the *Hs* DCP1 EVH1 domain (PDB code: 4B6H). (*C*) Structure of the *Sp* Dcp2 HLM1 bound to the Edc3 LSm domain (PDB code: 4A54). (*D*) Structure of the *Hs* EDC3 FDF motif bound to the C-terminal RecA-like domain of DDX6 (RecA-C) (PDB code: 2WAX). (*E*) *Sc* Edc3 binds patch 1 on Dhh1 RecA-C with its FDF sequence but also contacts patch 3 (PDB code: 4BRU). In this structure, binding of *Sc* Edc3 to patch 2 was not visible. (*F*) Structure of the *Sc* Pat1 N-terminal FDF motif bound to the RecA-C domain of *Sc* Dhh1. Pat binds patch 1 and displays extensive contacts to patch 3 near the RNA-binding site (PDB code: 4BRW). (*G*) Structure of the *Sc* LSm1–7 ring bound to Pat-C (PDB code: 4C8Q).

mediated mRNA decay pathway (NMD), which degrades aberrant mRNAs with nonsense codons (Lai et al. 2012).

The rapid evolution of DCP1 ligands is not surprising given that DCP1 recognizes short PRSs in protein partners. It is therefore possible that other proteins use the DCP1-binding groove to recruit the decapping complex or regulate its activity through a multilayered network of protein–protein interactions (Borja et al. 2011).

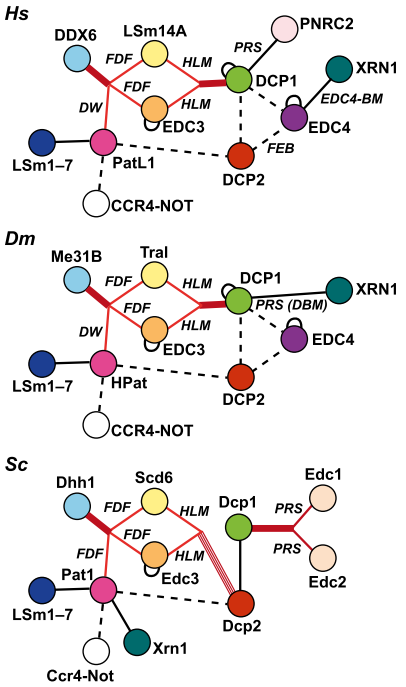

Figure 5. Evolutionary plasticity of the decapping network. Interaction networks between decapping factors in *Hs*, *Dm*, and *Sc* cells. Proteins are indicated as circles, labeled with their species-specific names, and colored according to Figures 1 and 3. Direct interactions are denoted by solid lines, and mutually exclusive interactions are highlighted in red. When the interactions are mediated by SLiMs, the motifs are indicated in italics. Dotted lines indicate interactions that have not yet been demonstrated to be direct. *Sc* Dcp2 has four HLM-bindings sites, shown by four red lines. Semicircles on DCP1 and EDC3 indicate oligomerization.

The LSm fold: a versatile scaffold for the assembly of multiprotein complexes

The (L)Sm (Sm and like Sm) fold is the most common fold present in decapping factors. It is present in the LSm1–7 proteins, EDC3 (LSm16) family proteins, and LSm14A and its orthologs (in *Sc*, Scd6 or LSm13; in *Dm*, Trailer hitch [Tral or LSm15]; and in *Caenorhabditis elegans*, CAR-1) (Fig. 3D–F; Albrecht and Lengauer 2004; Anantharaman and Aravind 2004). The Sm fold comprises an N-terminal α helix stacked on top of a strongly bent, five-stranded anti-parallel β sheet, which forms a barrel-like structure (Fig. 3D; Wilusz and Wilusz 2005).

(L)Sm proteins often oligomerize to form hexameric or heptameric rings that bind ssRNA. Ring formation is mediated by anti-parallel interactions between strand β4 of one subunit and strand β5 of the adjacent subunit (Fig. 3D). In contrast, RNA binding is mainly provided by residues in the loops that face the lumen of the ring (loops L3 and L5) (Fig. 3D; Leung et al. 2011). In the spliceosomal Sm ring, the RNA binds one face of the ring (the proximal face), and the 3′ end then threads through the central channel exiting on the opposite distal face of the ring (Leung et al. 2011).

The LSm1–7 proteins form a heptameric ring (Fig. 3D) that transiently interacts with cytoplasmic mRNAs and plays a role in the coordination of deadenylation and decapping through its interaction with Pat (Bouveret et al. 2000; Tharun et al. 2000; Tharun and Parker 2001; Sharif and Conti 2013; see below). Two structural features distinguish the LSm1–7 ring from other known Sm rings. One is a C-terminal extension in LSm2 that forms an α helix (α-2) that lies on the proximal face of the ring between LSm2 and LSm3 (Fig. 3D; Sharif and Conti 2013). The second and most striking feature is the C-terminal extension of LSm1, which forms a long α helix (α3) that folds back on the distal face of the ring and occludes the central channel (Fig. 3D). This LSm1 α3 helix might prevent (or constrain) threading of RNA molecules through the lumen of the ring (Sharif and Conti 2013).

In contrast to the LSm1–7 proteins, the LSm domains of the EDC3 and LSm14A proteins are flanked by long C-terminal extensions (Figs. 1, 3E,F; Albrecht and Lengauer 2004; Anantharaman and Aravind 2004). These C-terminal extensions feature a central FDF motif embedded in low-complexity regions rich in glycine and charged residues (Fig. 1; Albrecht and Lengauer 2004; Anantharaman and Aravind 2004; Kshirsagar and Parker 2004; Fenger-Grøn et al. 2005; Tanaka et al. 2006; Yang et al. 2006; Tritschler et al. 2007, 2008). Additionally, EDC3 proteins contain a conserved C-terminal YjeF-N domain that mediates homodimerization (Fig. 1, 3G; Ling et al. 2008).

Structural studies indicate that two of the hallmarks of canonical LSm proteins—i.e., ring formation and RNA-binding properties—are absent in the divergent LSm domains of EDC3 and LSm14A (Tritschler et al. 2007, 2008). As a result, these domains have acquired novel functionalities that appear to be conserved among their respective orthologs.

The EDC3 and LSm14A LSm domains recognize HLM motifs in protein partners

The LSm domains of metazoan EDC3 and LSm14A provide a binding surface for the DCP1 HLM motif, which consequently binds either EDC3 or LSm14A in a mutually exclusive manner (Tritschler et al. 2007, 2008). As previously mentioned, yeast DCP1 lacks a C-terminal extension and therefore does not contain an HLM (Fig. 1). In exchange, the long C-terminal extensions in *Sc* and *Sp* Dcp2 harbor six HLMs, of which four bind to yeast Edc3 or the LSm14A ortholog known as Scd6 (Harigaya et al. 2010; Fromm et al. 2012). HLM-1 flanks the Dcp2 Nudix domain and exhibits the highest affinity for Edc3 and Scd6, which consequently compete for binding to HLM-1 and the additional HLMs (Figs. 1, 2A; Fromm et al. 2012).

Sp Dcp2 HLM peptides are disordered in solution but fold into an amphipathic α helix upon binding to the *Sp* Edc3 LSm domain (Fig. 4C; Fromm et al. 2012). The HLM helix binds to β strands 2 and 5 of the LSm domain (Fig. 4C). This mode of interaction is possible only as a result of two specific features of the EDC3 (and LSm14A) LSm domains. First, these LSm domains remain monomeric; therefore, β strand 5, which is normally used for inter-

molecular contacts, is available for interaction with the N-terminal end of the HLM helix. Second, in contrast to canonical (L)Sm folds, the N-terminal helix is either absent or shorter in the EDC3 and LSm14A LSm domains (Fig. 3E,F vs. D), which makes space available for interaction with the C-terminal end of the HLM helix (Fig. 4C; Fromm et al. 2012).

The presence of multiple HLMs in the yeast Dcp2 C-terminal extension may increase the affinity of Dcp2 for yeast Edc3 or Scd6 (LSm14A) through avidity effects. In addition, because Edc3 dimerizes via its YjeF_N domain (Fig. 3G), each monomer can contact an HLM on Dcp2, eventually increasing the affinity of the interaction through cooperative effects. In metazoans, the HLM is present in DCP1, and avidity effects to recruit EDC3 could be achieved through DCP1 trimerization rather than the presence of multiple HLMs on a single polypeptide chain.

The relative affinity of the EDC3 and LSm14A LSm domains for HLMs has not been precisely determined, but available biochemical evidence suggests that the yeast and metazoan EDC3 bind HLMs with a higher affinity than LSm14A (Tritschler et al. 2008; Fromm et al. 2012). Consistent with its lower affinity, yeast Scd6 barely stimulates Dcp2 decapping activity in vitro (Fromm et al. 2012). In contrast, Edc3 stimulates Dcp2 decapping activity, but the underlying stimulatory mechanism is unknown, in particular because HLM-1 is not available for Edc3 (or Scd6) binding in the closed Dcp2 conformation (Fig. 2A; Fromm et al. 2012).

In summary, the specific and divergent features of the EDC3 and LSm14A LSm domains allow for the recognition of HLMs present in Dcp2 in yeast and DCP1 in metazoans (Figs. 3E,F, 4C, 5). The HLMs showcase how the convergent evolution of SLiMs rewires the decapping network.

EDC3, LSm14A, and Pat compete for binding to a common surface on DDX6

DDX6 is a DEAD-box protein that belongs to the large family of ATP-dependent RNA helicases. These proteins mediate RNA or RNA–protein structural rearrangements and play many roles in cellular RNA metabolism (Linder and Lasko 2006). Like all DEAD-box proteins, DDX6 consists of a conserved catalytic helicase core with two tandem RecA-like domains connected by a linker (Fig. 3H; Linder and Lasko 2006). The RecA-like domains adopt a typical α/β fold, which is characterized by a central six-stranded parallel β sheet sandwiched between α helices (Cheng et al. 2005).

Interaction studies have shown that the C-terminal RecA-like domain (RecA-C) of DDX6 orthologs provides binding sites for short related motifs present in EDC3, LSm14A, and Pat proteins, which therefore compete for DDX6 binding (Figs. 1, 5; Decker et al. 2007; Tritschler et al. 2007, 2008, 2009b; Braun et al. 2010; Haas et al. 2010; Sharif et al. 2013). While EDC3, LSm14A, and *Sc* Pat contain conserved FDF motifs, *Hs* and *Dm* Pat use a related DW motif for DDX6 binding (Figs. 1, 5).

Crystal structures of the EDC3 and Pat peptides bound to DDX6 from humans and yeast (known as *Sc* Dhh1) provide a mechanistic explanation for the competition of these motifs (Tritschler et al. 2009b; Sharif et al. 2013). A common feature of these SLiMs is that the aromatic rings of the phenylalanines in the FDF motif are accommodated in a hydrophobic pocket in DDX6 (patch 1 or FDF pocket) (Fig. 4D–F). This patch is also bound by the DW motif of *Hs* and *Dm* Pat (Haas et al. 2010; Sharif et al. 2013), providing the basis for the mutually exclusive binding to DDX6. Apart from this common binding site, neighboring sequences surrounding the FDF/DW motifs contact additional surfaces on DDX6. EDC3 contains short helices that fold upon binding to DDX6 and an FDK motif that occupies a second surface patch opposite the DDX6 surface involved in RNA binding (patch 2) (Fig. 4D,E). Mutational studies indicate that LSm14A proteins do not compete for patch 2 but could eventually contact other DDX6 surfaces (Tritschler et al. 2009b).

Notably, *Sc* Edc3 and Pat1 contact an additional surface on *Sc* Dhh1 (patch 3) that is positively charged and located in the vicinity of the canonical ATP-dependent RNA-binding surface (Fig. 4F). Binding is mediated through a stretch of negatively charged residues located N-terminal to the FDF motif that consequently interfere with Dhh1 binding to RNA (Sharif et al. 2013). These negatively charged residues are conserved in Pat orthologs (Fig. 4E); however, they are absent in metazoan EDC3 proteins, which are therefore unlikely to bind patch 3. Thus, Pat proteins and yeast Edc3 have the unexpected ability to release DDX6 (Dhh1) from RNA (Sharif et al. 2013). It will be important to ascertain how and when DDX6 release from RNA contributes to decapping.

Cumulatively, these studies indicate that a hydrophobic pocket in the RecA-C domain of DDX6 orthologs serves as a docking site for protein ligands containing FDF and DW motifs. Binding affinity and specificity are increased through additional contacts mediated by the flanking sequences. The FDF-binding pocket enables DDX6 to establish multiple and mutually exclusive interactions, assembling into distinct protein complexes. In these complexes, DDX6 proteins may act as remodeling subunits, and the final outcome of their activity (i.e., decapping or translational repression) will be specified by the additional components in the complexes (Tritschler et al. 2009b).

Coordination of decapping and deadenylation

The decapping of bulk mRNA in eukaryotes occurs after the mRNAs have been deadenylated. This order of events (deadenylation first, then decapping) ensures that functional, fully polyadenylated mRNAs are not prematurely decapped and degraded. However, how decapping and deadenylation are coordinated is poorly understood. Pat may play a role in mediating this coordination by interacting with decapping factors and components of the CCR4–NOT complex, the major cytoplasmic deadenylase complex in eukaryotic cells (Haas et al. 2010; Ozgur et al. 2010). Indeed, in all eukaryotic systems examined to date, Pat proteins interact with DCP2, DDX6, the LSm1–7

ring, and the CCR4–NOT complex (Bonnerot et al. 2000; Bouveret et al. 2000; Fromont-Racine et al. 2000; Tharun et al. 2000; Coller et al. 2001; Tharun and Parker 2001; Pilkington and Parker 2008; Tarassov et al. 2008; Braun et al. 2010; Haas et al. 2010; Marnef et al. 2010; Nissan et al. 2010; Ozgur et al. 2010).

As mentioned above, the interaction with DDX6 is mediated by the conserved N-terminal FDF/DW motif (Braun et al. 2010; Haas et al. 2010; Sharif et al. 2013). This motif is followed by a P-rich region, a middle (Mid) region, and a C-terminal domain termed Pat-C (Fig. 1). Pat-C is the only independently folding domain in Pat proteins in isolation (Braun et al. 2010). Pat-C folds into an α–α superhelix, exposing a conserved and basic patch on one side of the domain (Fig. 3B,C; Braun et al. 2010; Sharif and Conti 2013). In human cells, this conserved patch mediates binding to RNA, the LSm1–7 ring, DCP2, and EDC4 (Braun et al. 2010), raising the possibility of competitive or cooperative binding between RNA and protein partners. Accordingly, Pat-C plays a crucial role in decapping (Pilkington and Parker 2008; Braun et al. 2010; Haas et al. 2010; Nissan et al. 2010).

The binding site for the LSm1–7 ring in Pat proteins is bipartite; in addition to the conserved patch on Pat-C, a second binding site is located in the Mid region. The relative contribution of these binding sites to the affinity of the interaction differs between species (Pilkington and Parker 2008; Braun et al. 2010; Nissan et al. 2010; Sharif and Conti 2013). Structural information is available for the interaction mediated by the conserved patch on Pat-C. The conserved patch binds to the outer lateral side of the LSm1–7 ring, on a composite surface contributed by the LSm2 and LSm3 subunits. Upon binding, the Pat-C superhelix projects into the solvent like a handle (Sharif and Conti 2013). It has been suggested that a short motif in the Pat Mid region may contact an additional conserved surface on LSm2 (Sharif and Conti 2013).

Notably, studies using deletion mutants indicate that the P-rich region inhibits the binding of the LSm1–7 ring to the Mid region of *Dm* Pat, and this negative effect is counteracted by Pat-C (Braun et al. 2010). Although these observations cannot be explained in molecular terms, they suggest a complex interplay between Pat domains that may reflect different conformations of the protein: with and without affinity for LSm1–7. These data also suggest that the interaction between Pat and decapping factors may occur sequentially, allowing decapping complexes to assemble in a stepwise manner. This hypothesis is further supported by the observation that binding to DCP2/EDC4 and the LSm1–7 ring is mediated by the conserved patch on Pat-C, which is unlikely to accommodate all of these partners simultaneously (Braun et al. 2010; Nissan et al. 2010).

Interactions with components of the CCR4–NOT1 deadenylase complex have not been studied in detail, but multiple Pat domains contribute, including the P-rich and Mid regions, suggesting that these interactions are again mediated by disordered regions and could be difficult to tackle at the molecular level (Haas et al. 2010; Ozgur et al. 2010).

How does Pat coordinate decapping and deadenylation? Work from the past two decades has shown that the LSm1–7 complex preferentially binds to the 3′ end of oligoadenylated mRNAs that have undergone deadenylation, thereby protecting them from 3′ trimming and further degradation. Pat interacts with the LSm1–7 ring and is therefore recruited to deadenylated mRNAs (Bouveret et al. 2000; He and Parker 2001; Tharun and Parker 2001; Chowdhury et al. 2007; Pilkington and Parker 2008; Chowdhury and Tharun 2009). The interaction between Pat and the CCR4–NOT complex could also contribute to the recruitment of Pat to mRNAs undergoing deadenylation, providing a mechanism for coupling the removal of the mRNA poly(A) tail with decapping (Haas et al. 2010; Ozgur et al. 2010). Once recruited, the association between Pat and decapping factors would promote the assembly of decapping complexes in *cis*, committing deadenylated mRNAs to decapping and 5′-to-3′ mRNA degradation. During this process, Pat proteins may interact in a coordinated fashion with the CCR4–NOT complex, the LSm1–7 ring, and decapping factors, allowing transitions between sequential steps along the mRNA decay pathway (Braun et al. 2010).

SLiMs couple decapping to 5′-to-3′ degradation by XRN1

Decapping makes mRNA susceptible to degradation by the 5′-to-3′ exonuclease XRN1 (Arribas-Layton et al. 2013). A recent study indicated that decapping and XRN1-mediated degradation are coupled through direct interactions between XRN1 and decapping factors (Braun et al. 2012). This coupling provides an explanation for why decapped mRNAs are barely detectable in eukaryotic cells unless XRN1 activity is compromised.

XRN1 is a large protein consisting of a highly conserved N-terminal catalytic domain and a less conserved C-terminal region of variable length that is predicted to be predominantly disordered (Fig. 1; Chang et al. 2011; Jínek et al. 2011). This C-terminal region interacts with decapping factors, but the interactions have been rewired during eukaryotic evolution (Fig. 5; Braun et al. 2012).

In *Dm*, XRN1 interacts with the aromatic cleft in the DCP1 EVH1 domain through a PRS (or DBM) (Figs. 1, 4A). The structure of the *Dm* DCP1 EVH1 domain bound to the DBM revealed that the DBM peptide docks at the aromatic cleft and partially folds upon binding, forming an extended strand and a C-terminal α helix (Fig. 4A).

The motif present in *Dm* XRN1 is conserved in insects but not in nematodes and vertebrates, which is in agreement with the lack of conservation of the XRN1 C-terminal region. Nevertheless, the interaction between XRN1 and decapping factors as such is conserved in vertebrates. Indeed, the C-terminal region of vertebrate XRN1 has evolved the ability to bind EDC4 through a C-terminal motif termed the EDC4-binding motif (EDC4-BM) (Fig. 1; Braun et al. 2012). Thus, *Hs* EDC4 and *Dm* DCP1 mechanistically link DCP2 activation to mRNA degradation by providing a binding site for rapidly evolving SLiMs in the XRN1 C-terminal extension (Figs. 1, 5). In yeast, Xrn1 interacts with Pat1 (Bouveret et al. 2000;

Nissan et al. 2010), but the molecular details of this interaction are unknown.

The interaction between XRN1 and the decapping complex ensures that the enzyme is present at the location where the decapped mRNA is produced. Remarkably, XRN1 overexpression inhibits decapping in a dominant-negative manner in *Dm*, suggesting that an excess of XRN1 interferes with the assembly of active decapping complexes (Braun et al. 2012). Furthermore, XRN1 depletion reduces decapping efficiency, suggesting that a feedback mechanism ensures that decapping is not efficient if XRN1 is not in place (Braun et al. 2012). How XRN1 influences decapping remains to be elucidated.

Disordered regions mediate phase transitions driving RNP granule assembly

Decapping factors localize to P bodies and stress granules in somatic cells and to P granules and related RNP granules during oogenesis and embryogenesis as well as in neurons. These RNP granules contain a variety of proteins involved in mRNA degradation, translational repression, mRNA surveillance, and RNA-mediated gene silencing together with their mRNA targets (Eulalio et al. 2007a; Parker and Sheth 2007).

Recent studies shed new light on the specific mechanisms of RNP granule assembly and the role of decapping factors by demonstrating that these granules exhibit characteristics of liquid droplets, and their formation follows the principles of classical liquid–liquid phase separations (Brangwynne et al. 2009; Li et al. 2012; Weber and Brangwynne 2012). Two specific protein features are required for these transitions to occur: low-affinity interactions and multivalency of the interactions. These properties are common in RNA-binding proteins and have been demonstrated to be sufficient to induce phase separation into liquid droplets (Kato et al. 2012; Li et al. 2012). Furthermore, disordered, low-complexity protein regions are capable of inducing phase transitions, forming hydrogels (Han et al. 2012; Kato et al. 2012).

Although it is unclear whether RNP granules are more liquid-like or hydrogel-like in vivo, the properties required to promote these transitions are similar and are abundant in decapping factors. Their low-complexity regions are often rich in proline, glutamine, and asparagine (P/Q/N-rich) and have the ability to self-interact (Han et al. 2012; Kato et al. 2012). Proline residues could play a structural role by keeping these regions in an extended conformation, rendering short sequence motifs accessible for interaction with protein partners and providing multiple, nonspecific binding sites for protein–protein interactions (Williamson 1994). Multivalent binding is further ensured by homotypic interactions mediated by oligomerization domains (e.g., DCP1 trimerization and EDC3 dimerization) and heterotypic interactions mediated by SLiM mutimerization (e.g., HLMs in DCP2). In addition, decapping factors associate with RNA, and DDX6 at least has been shown to multimerize on RNA (Ernoult-Lange et al. 2012). These RNA molecules can be bridged through interactions mediated by EDC3 or DCP1 oligomerization domains, resulting in multivalent networks.

The molecular properties required for RNP granule assembly provide an explanation for why many granule components, including RNA, are required for granule integrity, and their depletion disperses the remaining components throughout the cytoplasm (Eulalio et al. 2007a; Parker and Sheth 2007). Indeed, phase transitions are dependent on the concentration of the individual components, and depleting one component can cause granule dissolution by lowering the concentration of components below the transition point (Brangwynne et al. 2009).

Photobleaching experiments have revealed that many P-body components are not stably bound but rather exchange rapidly with the cytoplasmic pool, indicating that the interactions that retain them in P bodies are weak and transient (Andrei et al. 2005; Kedersha et al. 2005; Leung et al. 2006; Aizer et al. 2008). Indeed, the retention time for proteins in specific granules depends on the strength of the interaction with granule components. Proteins that do not interact with granule components will rapidly diffuse through without being retained (Han et al. 2012; Kato et al. 2012). Further flexibility could be imparted by post-translational modifications that could modify retention times via modulation of protein–protein interactions. Thus, retention times and granule composition are expected to change depending on the cellular condition or cell type. As a result, the factors that are essential for granule formation and the signals required for the retention of specific proteins in these granules are not conserved. For example, the portion of the *Dm* Pat required for accumulation in P bodies is the P-rich region (Haas et al. 2010). In contrast, in *Sc* and human cells, Pat-C is required for Pat to localize in P bodies (Pilkington and Parker 2008; Braun et al. 2010).

What is the function of P bodies? P bodies are not sites for the storage of decay factors because most of these factors are diffusely distributed elsewhere in the cytoplasm, and less than ~10% of their cytoplasmic pool is actually localized in P bodies (Leung et al. 2006; Aizer et al. 2008). Furthermore, P bodies are not obligatory sites for translational repression and decay because their integrity is not required for bulk or sequence-specific mRNA degradation (Stoecklin et al. 2006; Decker et al. 2007; Eulalio et al. 2007b). Additionally, decay enzymes are also detected in polysomes, indicating that the sequestration of mRNA in P bodies is not a prerequisite for translational repression or decay (Hu et al. 2009). However, these studies do not rule out the possibility that P bodies may play a role in accelerating mRNA decay or facilitating the assembly of protein complexes due to the high local concentrations of enzymes and interacting partners. Additionally, P bodies and related granules may consolidate translational repression by excluding translation factors and ribosomes.

Mechanisms underlying functional and target specificity

A central question is how functional and target specificity is achieved despite the fact that decapping factors,

translational regulators, and mRNA targets coexist in P bodies. Functional specificity is favored by mutually exclusive interactions mediated by SLiMs competing for the same binding site in binding partners and promoting the assembly of distinct decapping complexes, which may act on specific mRNA targets. However, functional specificity might be opposed by the intrinsic property of decapping factors to form large multivalent networks that promote phase transitions and RNP granule formation.

Nevertheless, despite colocalizing to RNP granules, evidence from various organisms suggests that several mechanisms exist to enable decapping factors to assemble into functionally distinct complexes that act on specific targets. These mechanisms operate at the transcript level by inhibiting or activating decapping in a transcript-specific manner or more generally regulate the assembly of decapping complexes by modulating protein–protein interactions.

One striking example of how carefully choreographed interactions ensure functional specificity is provided by the related proteins EDC3 and LSm14A. Metazoan EDC3 and LSm14A compete for binding to common partners (DCP1 and DDX6) and colocalize to P bodies. However, EDC3 assembles in decapping complexes containing DCP1, DDX6, EDC4, and DCP2 (Fenger-Grøn et al. 2005; Tritschler et al. 2008), whereas *Dm* LSm14A associates with DDX6 (termed Me31B), DCP1, and the translational repressor CUP (Wilhelm et al. 2005; Tritschler et al. 2008). As a result, LSm14A-containing complexes are thought to repress translation in the absence of decapping in several eukaryotic organisms (Decker and Parker 2006; Nissan et al. 2010; Rajyaguru et al. 2012).

Although we are still far from being able to explain the selective assembly of these complexes and how LSm14A targets escape decapping, recent work has yielded initial clues. CUP is a eIF4E-binding protein that has the striking ability to inhibit the decapping of bound mRNAs, most likely by preventing DCP2 from accessing the cap structure (Igreja and Izaurralde 2011). Thus, through their association with CUP, LSm14A mRNA targets become impervious to decapping. CUP provides an example of a transcript-specific decapping inhibitor. Additional proteins that act as decapping inhibitors have been described and include the variable charged X chromosome (VCX)-A protein and YB-1 (Evdokimova et al. 2001; Jiao et al. 2006). Such mRNA-specific decapping inhibitors would be likely to play an important role in preventing unscheduled decapping. Additionally, some mRNAs can be recapped (Mukherjee et al. 2012), although the mechanisms involved remain elusive.

On the other hand, decapping can be activated in a transcript-specific manner. In NMD, DCP1 and DCP2 are recruited to mRNAs containing nonsense codons through interactions with the NMD effector UPF1 (Muhlrad and Parker 1994; He and Jacobson 2001). Similarly, DCP1 and DCP2 are recruited to mRNAs containing AU-rich elements (ARE) by ARE-binding proteins, such as TTP (tristetraprolin) (Fenger-Grøn et al. 2005). The ribosomal protein Rps28 and the export factor Yra1 recruit EDC3 and additional decapping factors to their own mRNA to autoregulate their own expression (Badis et al. 2004; Dong et al. 2010; Kolesnikova et al. 2013). Finally, decapping factors are recruited to miRNA targets via interactions with Argonaute complexes (Chu and Rana 2006; Barišić-Jäger et al. 2013; Nishihara et al. 2013). In the above examples, it is not known whether decapping is enhanced by increasing the local concentration of decapping factors or through direct effects on catalysis.

In addition to the mechanisms that operate at the transcript level, various additional mechanisms ensure that mRNAs are not precociously decapped. The simplest mechanism is the temporal and spatial regulation of decapping factor expression such that not all factors are coexpressed at the same time or in the same cells. For example, in immature mouse oocytes, DCP2 and DCP1 are not detectable, but their expression increases during oocyte maturation (Ma et al. 2013). As a result, in immature oocytes, maternal mRNAs will not be decapped, even if they localize with other decapping factors in RNP granules.

Alternatively, post-translational modifications can act as switches, favoring or disrupting particular interactions and regulating decapping complex and RNP granule composition. DCP1 and DCP2 are phosphorylated under cellular stress conditions (Yoon et al. 2010; Rzeczkowski et al. 2011; Xu and Chua 2012), and DCP1 is hyperphosphorylated during mitosis (Aizer et al. 2013). Under these conditions, a subset of mRNAs is stabilized, suggesting that the activity of decapping complexes can be regulated by phosphorylation. Additionally, it is possible that simple competition driven by differences in concentrations and cooperative effects favor the assembly of complexes and granules of defined composition and function.

Outlook

Despite the wealth of available information, key questions regarding the assembly and regulation of decapping remain unanswered. Perhaps the most urgent question concerns the conformation of the catalytically active form of the decapping enzyme. This information will be required for a molecular understanding of DCP2 activation by DCP1, which in turn will provide important insight into how PRS ligands (e.g., Edc1, Edc2, XRN1, and PNRC2) influence DCP2 activity. DCP1 has been shown to promote the closed active conformation of DCP2, which is then consolidated by Edc1 (Floor et al. 2012). Do all DCP1 ligands operate according to a similar principle or only use the DCP1 aromatic cleft to dock on the decapping complex and mediate different effects?

Emerging evidence suggests that decapping involves consecutive steps in which protein–protein interactions are formed and disrupted in a coordinated fashion. However, our knowledge of these interactions is static, and the mechanism allowing sequential interactions to occur (conformational changes, activity of RNA helicases, and post-translational modifications) remain largely unexplored.

The coordination of early steps in eukaryotic gene expression is well documented (e.g., mRNA transcription and processing) and is mediated by direct molecular interactions of the involved components. However, little

is known about the molecular mechanisms that couple decapping with other post-transcriptional processes, including translational repression, deadenylation, and 5′-to-3′ mRNA decay. Decapping and translation machineries compete for mRNA access, and decapping activators (i.e., DDX6, Pat, and LSm14A) repress translation (Coller and Parker 2005; Marnef et al. 2010; Nissan et al. 2010; Rajyaguru et al. 2012; Sweet et al. 2012); however, their molecular mechanisms have not been fully elucidated.

Equally interesting is the connection between decapping complexes and other cellular processes. Considering that eukaryotic cells code for multiple decapping activators and that the globular domains of these activators provide binding sites for SLiMs in binding partners, it is conceivable that these activators interact with additional unidentified ligands. The aromatic cleft of the DCP1 EVH1 domain, the hydrophobic pocket of DDX6, and the HLM-binding surface of the EDC3 and LSm14A LSm domains may provide binding sites for additional protein partners. These proteins may hook into the decapping complex to coordinate DCP2 activation with other cellular processes or may recruit decapping complexes to specific RNA targets.

Decapping complexes were thought to be expressed and function in the cytoplasm. The recent discovery that the DCP2–DCP1–EDC3 complex plays a role in nuclear RNA degradation (Brannan et al. 2012; Geisler et al. 2012) raises the possibility that additional unidentified regulatory factors modulate DCP2 activity and its recruitment in the nuclear compartment. Understanding how DCP2 can properly navigate among its numerous interactors to ensure that decapping does not inadvertently occur while ensuring that the proper RNAs are decapped represents a challenging question for future studies.

Acknowledgments

We are grateful to O. Weichenrieder for insightful comments on the manuscript. The research from this laboratory is supported by the Max Planck Society and grants from the Deutsche Forschungsgemeinschaft (DFG, FOR855, and the Gottfried Wilhelm Leibniz Program awarded to E.I.) and the European Union Seventh Framework Programme through a Marie Curie Fellowship (FP7, no. 275343 to S.J.).

References

Albrecht M, Lengauer T. 2004. Novel Sm-like proteins with long C-terminal tails and associated methyltransferases. *FEBS Lett* **569:** 18–26.

Anantharaman V, Aravind L. 2004. Novel conserved domains in proteins with predicted roles in eukaryotic cell-cycle regulation, decapping and RNA stability. *BMC Genomics* **5:** 45.

Andrei MA, Ingelfinger D, Heintzmann R, Achsel T, Rivera-Pomar R, Lührmann R. 2005. A role for eIF4E and eIF4E-transporter in targeting mRNPs to mammalian processing bodies. *RNA* **11:** 717–727.

Aizer A, Brody Y, Ler LW, Sonenberg N, Singer RH, Shav-Tal Y. 2008. The dynamics of mammalian P body transport, assembly, and disassembly in vivo. *Mol Biol Cell* **19:** 4154–4166.

Aizer A, Kafri P, Kalo A, Shav-Tal Y. 2013. The P body protein Dcp1a is hyper-phosphorylated during mitosis. *PLoS ONE* **8:** e49783.

Arribas-Layton M, Wu D, Lykke-Andersen J, Song H. 2013. Structural and functional control of the eukaryotic mRNA decapping machinery. *Biochim Biophys Acta* **1829:** 580–589.

Badis G, Saveanu C, Fromont-Racine M, Jacquier A. 2004. Targeted mRNA degradation by deadenylation-independent decapping. *Mol Cell* **15:** 5–15.

Barišić-Jäger E, Kręcioch I, Hosiner S, Antic S, Dorner S. 2013. HPat a decapping activator interacting with the miRNA effector complex. *PLoS ONE* **8:** e71860.

Bloch DB, Nobre RA, Bernstein GA, Yang WH. 2011. Identification and characterization of protein interactions in the mammalian mRNA processing body using a novel two-hybrid assay. *Exp Cell Res* **317:** 2183–2199.

Bonnerot C, Boeck R, Lapeyre B. 2000. The two proteins Pat1p (Mrt1p) and Spb8p interact in vivo, are required for mRNA decay, and are functionally linked to Pab1p. *Mol Cell Biol* **20:** 5939–5946.

Borja MS, Piotukh K, Freund C, Gross JD. 2011. Dcp1 links coactivators of mRNA decapping to Dcp2 by proline recognition. *RNA* **17:** 278–290.

Bouveret E, Rigaut G, Shevchenko A, Wilm M, Seraphin B. 2000. A Sm-like protein complex that participates in mRNA degradation. *EMBO J* **19:** 1661–1671.

Brangwynne CP, Eckmann CR, Courson DS, Rybarska A, Hoege C, Gharakhani J, Jülicher F, Hyman AA. 2009. Germline P granules are liquid droplets that localize by controlled dissolution/condensation. *Science* **324:** 1729–1732.

Brannan K, Kim H, Erickson B, Glover-Cutter K, Kim S, Fong N, Kiemele L, Hansen K, Davis R, Lykke-Andersen J, et al. 2012. mRNA decapping factors and the exonuclease Xrn2 function in widespread premature termination of RNA polymerase II transcription. *Mol Cell* **46:** 311–324.

Braun JE, Tritschler F, Haas G, Igreja C, Truffault V, Weichenrieder O, Izaurralde E. 2010. The C-terminal α–α superhelix of Pat is required for mRNA decapping in metazoa. *EMBO J* **29:** 2368–2380.

Braun JE, Truffault V, Boland A, Huntzinger E, Chang CT, Haas G, Weichenrieder O, Coles M, Izaurralde E. 2012. A direct interaction between DCP1 and XRN1 couples mRNA decapping to 5′ exonucleolytic degradation. *Nat Struct Mol Biol* **19:** 1324–1331.

Chang JH, Xiang S, Xiang K, Manley JL, Tong L. 2011. Structural and biochemical studies of the 5′ → 3′ exoribonuclease Xrn1. *Nat Struct Mol Biol* **18:** 270–276.

Cheng Z, Coller J, Parker R, Song H. 2005. Crystal structure and functional analysis of DEAD-box protein Dhh1p. *RNA* **11:** 1258–1270.

Chowdhury A, Tharun S. 2009. Activation of decapping involves binding of the mRNA and facilitation of the post-binding steps by the Lsm1–7–Pat1 complex. *RNA* **15:** 1837–1848.

Chowdhury A, Mukhopadhyay J, Tharun S. 2007. The decapping activator Lsm1p–7p–Pat1p complex has the intrinsic ability to distinguish between oligoadenylated and polyadenylated RNAs. *RNA* **13:** 998–1016.

Chu CY, Rana TM. 2006. Translation repression in human cells by microRNA-induced gene silencing requires RCK/p54. *PLoS Biol* **4:** e210.

Coller J, Parker R. 2005. General translational repression by activators of mRNA decapping. *Cell* **122:** 875–886.

Coller JM, Tucker M, Sheth U, Valencia-Sanchez MA, Parker R. 2001. The DEAD box helicase, Dhh1p, functions in mRNA decapping and interacts with both the decapping and deadenylase complexes. *RNA* **7:** 1717–1727.

Davey NE, Van Roey K, Weatheritt RJ, Toedt G, Uyar B, Altenberg B, Budd A, Diella F, Dinkel H, Gibson TJ. 2012. Attributes of short linear motifs. *Mol Biosyst* **8:** 268–281.

Decker CJ, Parker R. 2006. CAR-1 and trailer hitch: Driving mRNP granule function at the ER? *J Cell Biol* **173:** 159–163.
Decker CJ, Teixeira D, Parker R. 2007. Edc3p and a glutamine/asparagine-rich domain of Lsm4p function in processing body assembly in *Saccharomyces cerevisiae*. *J Cell Biol* **179:** 437–449.
Deshmukh MV, Jones BN, Quang-Dang DU, Flinders J, Floor SN, Kim C, Jemielity J, Kalek M, Darzynkiewicz E, Gross JD. 2008. mRNA decapping is promoted by an RNA-binding channel in Dcp2. *Mol Cell* **29:** 324–336.
Dong S, Jacobson A, He F. 2010. Degradation of YRA1 pre-mRNA in the cytoplasm requires translational repression, multiple modular intronic elements, Edc3p, and Mex67p. *PLoS Biol* **8:** e1000360.
Ernoult-Lange M, Baconnais S, Harper M, Minshall N, Souquere S, Boudier T, Bénard M, Andrey P, Pierron G, Kress M, et al. 2012. Multiple binding of repressed mRNAs by the P-body protein Rck/p54. *RNA* **18:** 1702–1715.
Eulalio A, Behm-Ansmant I, Izaurralde E. 2007a. P bodies: At the crossroads of post-transcriptional pathways. *Nat Rev Mol Cell Biol* **8:** 9–22.
Eulalio A, Behm-Ansmant I, Schweizer D, Izaurralde E. 2007b. P-body formation is a consequence, not the cause of RNA-mediated gene silencing. *Mol Cell Biol* **27:** 3970–3981.
Evdokimova V, Ruzanov P, Imataka H, Raught B, Svitkin Y, Ovchinnikov LP, Sonenberg N. 2001. The major mRNA-associated protein YB-1 is a potent 5′ cap-dependent mRNA stabilizer. *EMBO J* **20:** 5491–5502.
Fenger-Grøn M, Fillman C, Norrild B, Lykke-Andersen J. 2005. Multiple processing body factors and the ARE binding protein TTP activate mRNA decapping. *Mol Cell* **20:** 905–915.
Floor SN, Jones BN, Hernandez GA, Gross JD. 2010. A split active site couples cap recognition by Dcp2 to activation. *Nat Struct Mol Biol* **17:** 1096–1101.
Floor SN, Borja MS, Gross JD. 2012. Interdomain dynamics and coactivation of the mRNA decapping enzyme Dcp2 are mediated by a gatekeeper tryptophan. *Proc Natl Acad Sci* **109:** 2872–2877.
Fromm SA, Truffault V, Kamenz J, Braun JE, Hoffmann NA, Izaurralde E, Sprangers R. 2012. The structural basis of Edc3- and Scd6-mediated activation of the Dcp1:Dcp2 mRNA decapping complex. *EMBO J* **31:** 279–290.
Fromont-Racine M, Mayes AE, Brunet-Simon A, Rain JC, Colley A, Dix I, Decourty L, Joly N, Ricard F, Beggs JD, et al. 2000. Genome-wide protein interaction screens reveal functional networks involving Sm-like proteins. *Yeast* **17:** 95–110.
Geisler S, Lojek L, Khalil AM, Baker KE, Coller J. 2012. Decapping of long noncoding RNAs regulates inducible genes. *Mol Cell* **45:** 279–291.
Haas G, Braun JE, Igreja C, Tritschler F, Nishihara T, Izaurralde E. 2010. HPat provides a link between deadenylation and decapping in metazoa. *J Cell Biol* **189:** 289–302.
Han TW, Kato M, Xie S, Wu LC, Mirzaei H, Pei J, Chen M, Xie Y, Allen J, Xiao G, et al. 2012. Cell-free formation of RNA granules: Bound RNAs identify features and components of cellular assemblies. *Cell* **149:** 768–779.
Harigaya Y, Jones BN, Muhlrad D, Gross JD, Parker R. 2010. Identification and analysis of the interaction between Edc3 and Dcp2 in *Saccharomyces cerevisiae*. *Mol Cell Biol* **30:** 1446–1456.
He F, Jacobson A. 2001. Upf1p, Nmd2p, and Upf3p regulate the decapping and exonucleolytic degradation of both nonsense-containing mRNAs and wild-type mRNAs. *Mol Cell Biol* **21:** 1515–1530.
He W, Parker R. 2001. The yeast cytoplasmic LsmI/Pat1p complex protects mRNA 3′ termini from partial degradation. *Genetics* **158:** 1445–1455.
Hu W, Sweet TJ, Chamnongpol S, Baker KE, Coller J. 2009. Co-translational mRNA decay in *Saccharomyces cerevisiae*. *Nature* **461:** 225–229.
Igreja C, Izaurralde E. 2011. CUP promotes deadenylation and inhibits decapping of mRNA targets. *Genes Dev* **25:** 1955–1967.
Jiao X, Wang Z, Kiledjian M. 2006. Identification of an mRNA-decapping regulator implicated in X-linked mental retardation. *Mol Cell* **24:** 713–722.
Jínek M, Eulalio A, Lingel A, Helms S, Conti E, Izaurralde E. 2008. The C-terminal region of Ge-1 presents conserved structural features required for P-body localization. *RNA* **14:** 1991–1998.
Jínek M, Coyle SM, Doudna JA. 2011. Coupled 5′ nucleotide recognition and processivity in Xrn1-mediated mRNA decay. *Mol Cell* **41:** 600–608.
Kato M, Han TW, Xie S, Shi K, Du X, Wu LC, Mirzaei H, Goldsmith EJ, Longgood J, Pei J, et al. 2012. Cell-free formation of RNA granules: Low complexity sequence domains form dynamic fibers within hydrogels. *Cell* **149:** 753–767.
Kedersha N, Stoecklin G, Ayodele M, Yacono P, Lykke-Andersen J, Fritzler MJ, Scheuner D, Kaufman RJ, Golan DE, Anderson P. 2005. Stress granules and processing bodies are dynamically linked sites of mRNP remodeling. *J Cell Biol* **169:** 871–884.
Kolesnikova O, Back R, Graille M, Séraphin B. 2013. Identification of the Rps28 binding motif from yeast Edc3 involved in the autoregulatory feedback loop controlling RPS28B mRNA decay. *Nucleic Acids Res* **41:** 9514–9523.
Kshirsagar M, Parker R. 2004. Identification of Edc3p as an enhancer of mRNA decapping in *Saccharomyces cerevisiae*. *Genetics* **166:** 729–739.
Lai T, Cho H, Liu Z, Bowler MW, Piao S, Parker R, Kim YK, Song H. 2012. Structural basis of the PNRC2-mediated link between mRNA surveillance and decapping. *Structure* **20:** 2025–2037.
Leung AK, Calabrese JM, Sharp PA. 2006. Quantitative analysis of Argonaute protein reveals microRNA-dependent localization to stress granules. *Proc Natl Acad Sci* **103:** 18125–18130.
Leung AKW, Nagai K, Li J. 2011. Structure of the spliceosomal U4 snRNP core domain and its implication for snRNP biogenesis. *Nature* **473:** 536–539.
Li P, Banjade S, Cheng HC, Kim S, Chen B, Guo L, Llaguno M, Hollingsworth JV, King DS, Banani SF, et al. 2012. Phase transitions in the assembly of multivalent signalling proteins. *Nature* **483:** 336–340.
Linder P, Lasko P. 2006. Bent out of shape: RNA unwinding by the DEAD-box helicase Vasa. *Cell* **125:** 219–221.
Ling SH, Decker CJ, Walsh MA, She M, Parker R, Song H. 2008. Crystal structure of human Edc3 and its functional implications. *Mol Cell Biol* **28:** 5965–5976.
Lykke-Andersen J. 2002. Identification of a human decapping complex associated with hUpf proteins in nonsense-mediated decay. *Mol Cell Biol* **22:** 8114–8121.
Ma J, Flemr M, Strnad H, Svoboda P, Schultz RM. 2013. Maternally recruited DCP1A and DCP2 contribute to messenger RNA degradation during oocyte maturation and genome activation in mouse. *Biol Reprod* **88:** 11.
Marnef A, Maldonado M, Bugaut A, Balasubramanian S, Kress M, Weil D, Standart N. 2010. Distinct functions of maternal and somatic Pat1 protein paralogs. *RNA* **16:** 2094–2107.

Muhlrad D, Parker R. 1994. Premature translational termination triggers mRNA decapping. *Nature* **370:** 578–581.

Mukherjee C, Patil DP, Kennedy BA, Bakthavachalu B, Bundschuh R, Schoenberg DR. 2012. Identification of cytoplasmic capping targets reveals a role for cap homeostasis in translation and mRNA stability. *Cell Rep* **2:** 674–684.

Nishihara T, Zekri L, Braun JE, Izaurralde E. 2013. miRISC recruits decapping factors to miRNA targets to enhance their degradation. *Nucleic Acids Res* **41:** 8692–8705.

Nissan T, Rajyaguru P, She M, Song H, Parker R. 2010. Decapping activators in *Saccharomyces cerevisiae* act by multiple mechanisms. *Mol Cell* **39:** 773–783.

Ozgur S, Chekulaeva M, Stoecklin G. 2010. Human Pat1b connects deadenylation with mRNA decapping and controls the assembly of processing bodies. *Mol Cell Biol* **30:** 4308–4323.

Parker R, Sheth U. 2007. P bodies and the control of mRNA translation and degradation. *Mol Cell* **25:** 635–646.

Pilkington GR, Parker R. 2008. Pat1 contains distinct functional domains that promote P-body assembly and activation of decapping. *Mol Cell Biol* **28:** 1298–1312.

Rajyaguru P, She M, Parker R. 2012. Scd6 targets eIF4G to repress translation: RGG motif proteins as a class of eIF4G-binding proteins. *Mol Cell* **45:** 244–254.

Rzeczkowski K, Beuerlein K, Müller H, Dittrich-Breiholz O, Schneider H, Kettner-Buhrow D, Holtmann H, Kracht M. 2011. c-Jun N-terminal kinase phosphorylates DCP1a to control formation of P bodies. *J Cell Biol* **194:** 581–596.

Sharif H, Conti E. 2013. Architecture of the Lsm1–7–Pat1 complex: A conserved assembly in eukaryotic mRNA turnover. *Cell Rep* **5:** 283–291.

Sharif H, Ozgur S, Sharma K, Basquin C, Urlaub H, Conti E. 2013. Structural analysis of the yeast Dhh1–Pat1 complex reveals how Dhh1 engages Pat1, Edc3 and RNA in mutually exclusive interactions. *Nucleic Acids Res* **41:** 8377–8390.

She M, Decker CJ, Sundramurthy K, Liu Y, Chen N, Parker R, Song H. 2004. Crystal structure of Dcp1p and its functional implications in mRNA decapping. *Nat Struct Mol Biol* **11:** 249–256.

She M, Decker CJ, Chen N, Tumati S, Parker R, Song H. 2006. Crystal structure and functional analysis of Dcp2p from *Schizosaccharomyces pombe*. *Nat Struct Mol Biol* **13:** 63–70.

She M, Decker CJ, Svergun DI, Round A, Chen N, Muhlrad D, Parker R, Song H. 2008. Structural basis of dcp2 recognition and activation by dcp1. *Mol Cell* **29:** 337–349.

Stoecklin G, Mayo T, Anderson P. 2006. ARE-mRNA degradation requires the 5′–3′ decay pathway. *EMBO Rep* **7:** 72–77.

Sweet T, Kovalak C, Coller J. 2012. The DEAD-box protein Dhh1 promotes decapping by slowing ribosome movement. *PLoS Biol* **10:** e1001342.

Tanaka KJ, Ogawa K, Takagi M, Imamoto N, Matsumoto K, Tsujimoto M. 2006. RAP55, a cytoplasmic mRNP component, represses translation in *Xenopus* oocytes. *J Biol Chem* **281:** 40096–40106.

Tarassov K, Messier V, Landry CR, Radinovic S, Serna Molina MM, Shames I, Malitskaya Y, Vogel J, Bussey H, Michnick SW. 2008. An in vivo map of the yeast protein interactome. *Science* **320:** 1465–1470.

Tharun S, Parker R. 2001. Targeting an mRNA for decapping: Displacement of translation factors and association of the Lsm1p–7p complex on deadenylated yeast mRNAs. *Mol Cell* **8:** 1075–1083.

Tharun S, He W, Mayes AE, Lennertz P, Beggs JD, Parker R. 2000. Yeast Sm-like proteins function in mRNA decapping and decay. *Nature* **404:** 515–518.

Tompa P. 2012. Intrinsically disordered proteins: A 10-year recap. *Trends Biochem Sci* **37:** 509–516.

Tritschler F, Eulalio A, Truffault V, Hartmann MD, Helms S, Schmidt S, Coles M, Izaurralde E, Weichenrieder O. 2007. A divergent Sm fold in EDC3 proteins mediates DCP1 binding and P-body targeting. *Mol Cell Biol* **27:** 8600–8611.

Tritschler F, Eulalio A, Helms S, Schmidt S, Coles M, Weichenrieder O, Izaurralde E, Truffault V. 2008. Similar modes of interaction enable Trailer Hitch and EDC3 to associate with DCP1 and Me31B in distinct protein complexes. *Mol Cell Biol* **28:** 6695–6708.

Tritschler F, Braun JE, Motz C, Igreja C, Haas G, Truffault V, Izaurralde E, Weichenrieder O. 2009a. DCP1 forms asymmetric trimers to assemble into active mRNA decapping complexes in metazoa. *Proc Natl Acad Sci* **106:** 21591–21596.

Tritschler F, Braun JE, Eulalio A, Truffault V, Izaurralde E, Weichenrieder O. 2009b. Structural basis for the mutually exclusive anchoring of P body components EDC3 and Tral to the DEAD box protein DDX6/Me31B. *Mol Cell* **33:** 661–668.

van Dijk E, Cougot N, Meyer S, Babajko S, Wahle E, Seraphin B. 2002. Human Dcp2: A catalytically active mRNA decapping enzyme located in specific cytoplasmic structures. *EMBO J* **21:** 6915–6924.

Wang Z, Jiao X, Carr-Schmid A, Kiledjian M. 2002. The hDcp2 protein is a mammalian mRNA decapping enzyme. *Proc Natl Acad Sci* **99:** 12663–12668.

Wang CY, Chen WL, Wang SW. 2013. Pdc1 functions in the assembly of P bodies in *Schizosaccharomyces pombe*. *Mol Cell Biol* **33:** 1244–1253.

Weber SC, Brangwynne CP. 2012. Getting RNA and protein in phase. *Cell* **149:** 1188–1191.

Wilhelm JE, Buszczak M, Sayles S. 2005. Efficient protein trafficking requires trailer hitch, a component of a ribonucleoprotein complex localized to the ER in *Drosophila*. *Dev Cell* **9:** 675–685.

Williamson MP. 1994. The structure and function of proline-rich regions in proteins. *Biochem J* **297:** 249–260.

Wilusz CJ, Wilusz J. 2005. Eukaryotic Lsm proteins: Lessons from bacteria. *Nat Struct Mol Biol* **12:** 1031–1036.

Xu J, Chua NH. 2012. Dehydration stress activates *Arabidopsis* MPK6 to signal DCP1 phosphorylation. *EMBO J* **31:** 1975–1984.

Xu J, Yang JY, Niu QW, Chua NH. 2006. *Arabidopsis* DCP2, DCP1, and VARICOSE form a decapping complex required for postembryonic development. *Plant Cell* **18:** 3386–3398.

Yang WH, Yu JH, Gulick T, Bloch KD, Bloch DB. 2006. RNA-associated protein 55 (RAP55) localizes to mRNA processing bodies and stress granules. *RNA* **12:** 547–554.

Yoon JH, Choi EJ, Parker R. 2010. Dcp2 phosphorylation by Ste20 modulates stress granule assembly and mRNA decay in *Saccharomyces cerevisiae*. *J Cell Biol* **189:** 813–827.

Yu JH, Yang WH, Gulick T, Bloch KD, Bloch DB. 2005. Ge-1 is a central component of the mammalian cytoplasmic mRNA processing body. *RNA* **11:** 1795–1802.